

A Design Study and Performance Prediction of an Internal Compression Supersonic Air Intake

Bahjat Hassan Alyas

Technical College /Mosul

Email: Hai_Has_2009@yahoo.com

Received on: 8/3/2012 & Accepted on: 7/3/2013

ABSTRACT

The aim of this research is to carryout a design study on a variable geometry rectangular supersonic air-intake at different flight conditions. The design of the air-intake at supersonic Mach number according to “on-design” condition ($M_{\infty} = 2.0, H = 10000m$), to get a maximum total-pressure recovery, and study the performance of air-intake at supersonic Mach number according to “off-design” conditions ($M_{\infty} = 1.6 - 2.5$). The air-intake consists of convergent-divergent nozzle. The number of oblique shock waves is induced by the sharp cowl lips at the nozzle entrance and their reflections may continue along the convergent passage depending on the free-stream Mach number and nozzle wall turning angle. The location of the normal shock wave is just downstream the throat, for an “off-design” condition, and at nozzle throat, at its “on-design” condition [21]. The flow is assumed as one-dimensional compressible, and inviscid. The flow properties were calculated using the analytical method based on the relation of the oblique shock and normal shock waves. The divergent part was analyzed for different divergent lengths, to maintain the divergent angle less than value that causes flow separation and to get the maximum total pressure recovery. The convergent part was analyzed for different convergent lengths, to maintain the oblique shock and their reflected terminated before the throat position to get maximum total pressure recovery, [21].

Keywords: Convergent-Divergent Nozzle, Supersonic Air Intake, Normal and Oblique Shock Waves.

دراسة تصميمية وتخمين أداء لآخذة هواء فوق الصوتية تعمل بمبدأ الانضغاط الداخلي

الخلاصة

في هذه البحث تم دراسة تصميم آخذة هواء فوق الصوتية تعمل بمبدأ الانضغاط الداخلي لعدة ظروف جوية مختلفة. وهذا يشمل تصميم الآخذة عند ظروف تصميمية ($M_{\infty} = 2.0, H = 10000m$) للحصول على أكبر ضغط إرجاعي، ودراسة أداء الآخذة لظروف جوية غير تصميمية. يتألف هذا الجزء من منفث ملتئم-منفج يعمل بسرعه فوق صوتية عالية. إن عدد موجات الصدمات المائلة المحتثة بواسطة مدخل الآخذة الحاد وانعكاساتها ربما تستمر على طول الممر الملتئم معتمدا على رقم ماخ الجريان الحر وزاوية استدارة جدار الناشر. إن موقع موجة

الصدمة العمودية مباشرة ما بعد موقع العنق للظروف اللاتصميمية، وعند عنق الناشر للظروف التصميمية تم حسابها من علاقات الصدمات العمودية والمائلة. تم افتراض الجريان على أنه انضغاطي، غير لزج، أحادي البعد. استخدمت الطريقة التحليلية لحساب خواص الجريان مبنياً على علاقات موجات الصدمة المائلة والصدمة العمودية. حل الجزء المنفرج لعدة أطوال منفرجة لإبقاء زاوية الانفرج أقل من القيمة المسببة لانفصال الجريان. كما حل الجزء الملتئم لعدة أطوال لإبقاء الصدمة المائلة وانعكاساتها تتلاشى ما قبل موقع العنق لتجنب تشوه الجريان وللحصول على أكبر ضغط كلي إرجاعي.

INTRODUCTION

The prediction of flow in air intake is based on a practical importance in the development and design of air intake. So a large number of studies has been done to analyze the characteristics of flow field as follows.

A supersonic wind tunnel was investigated in the NACA Lewis 18×18 inch for the optimum design configurations for a convergent-divergent type of supersonic nozzle with a subsonic nozzle of 5° included divergence angle at a Mach number of 1.85 and at angles of attack from 0° to 5° , [1].

The perforated convergent-divergent supersonic nozzle was investigated for the total pressure recovery and characteristics of operating with initial boundary layer has been conducted at a Mach number of 1.90 at NACA Lewis laboratory, [2].

An oblique-shock nozzle (supersonic nozzle) was investigated how the should work, and where the oblique-shocks should intersect and reflect. The oblique-shocks angles and their relation had been described to deal with the wall angle if the first shock is reflected or intersected, [3].

A variable geometry inlet in combination with a J34 turbojet engine had been inspected in the experimental investigation on Mach number 2.0 of shock positioning control system. The shock-positioning controls designed to actuate the variable bypass of variable geometry inlet were investigated in the 8-by 6-foot supersonic wind tunnel. The operation of this inlet was observed in combination with a J34 Turbojet engine at tunnel Mach number from 1.7 to 2.0, [4].

The circular internal-compression inlets with translating center bodies was investigated for the total pressure recovery characteristics at free-stream Mach numbers from 2.1 to 3.0 at 0° angle of attack. Each of the inlets had the same ratio of the minimum area to the entrance area ($A_t/A_c=0.39$) at the design Mach number 2.5. The three inlets differed only in the shape of the internal compression contours, [5].

A variable internal contraction inlet has been studied for the performance of without boundary layer removal at Mach number 2.0, 2.5, and 2.92. The total pressure recovery at the design Mach number 2.5 was 0.78. At Mach number 2.0 and 2.92 the maximum total pressure ratios were 0.87 and 0.54, respectively, [6].

A single and double-oblique and conical-shock inlets were presented for the design charts for Mach numbers up to 4, for isentropic axi-symmetric and two-dimensional surfaces having theoretically focused Mach lines. The investigations concentrate solely on supersonic portion of air intake and the subsonic portion, especially the experimental and some of numerical investigations. Also some of the results of these investigations cover the variation of mass flow ratio with total pressure recovery and ignore the effect of other properties of flow, [7].

The air intake reduces free stream air speed and converts kinetic energy to pressure energy terms. On the increment of exhaust velocity, the static pressure of entrance air has a significant role in the engine efficiency improvement,[8].

The other method to obtain high pressure recovery is used of multiple oblique shocks with special arrangement. Usually use oblique shock to diffusing in stream for Mach 1.5 to 3.5 that lead to product a low weight geometry and desirable pressure recovery than isentropic design. An American scientists of NACA have a good research for bookmark and tales supersonic ramjet

Missile,[9].

In 2002, flow stability test in axisymmetric dual Y shape intake in mach 1.6 accomplished with Indian aeronautic department. In this test, several aspect ratios were considered experimentally,[10].

In 2006, study of flow filed in the entrance of a supersonic turbojet engine was performed by "Joe Iannelli" in aeronautic research university. In these numerical studies, flow filed was simulated steady and unsteady and fluid equation has been solved with and without (Euler equation) viscosity effect. The main goal of this research is optimization of supersonic diffuser design in mach 2 with 1 Kg/s of flow rate,[11].

The preliminary design of the silent supersonic technology demonstrator, S3TD, has been done in Japan Aerospace Exploration Agency, JAXA. S3TD is an experimental unmanned air vehicle. The one of the main object of developing the demonstrator is to validate the unique design technology for the reduction of

sonic boom in supersonic flight. In order to minimize the effect of the propulsion system, such as exhaust jet or spillage flow, on the characteristics of sonic boom, top mounted propulsion system was adopted to S3TD,[12].

CFD analysis was employed to evaluate inlet performances. Especially, the estimation of the external drag of the inlet, which is thought to be difficult to evaluate by wind tunnel tests, is expected. Three dimensional N-S equation was solved by CFD method including turbulence model using unique boundary condition, [13].

The purpose of this paper is to design and performance prediction of air-intake at different Mach numbers, that includes: - 1. Preliminary to design the supersonic air intake at high supersonic Mach number ($M_\infty > 1.5$) according to "on-design" condition ($M_\infty = 2.0, H = 10000m$), to get a maximum pressure recovery, 2. study the performance of a variable geometry rectangular supersonic air intake at different flight conditions according to "off-design" condition ($M_\infty = 1.6 - 2.5$).

METHODOLOGY

The supersonic air intake is considered as a variable geometry, rectangular internal compression intake with two internal facing ramps, achieving compression through a series of internal oblique shock waves followed by a terminal normal shock positioned downstream of the throat at high supersonic Mach number ($M_\infty > 1.5$) as shown in Figures. (1) and (2). This type of air intake requires a variable throat area to allow the inlet to swallow the normal shock at different operational Mach numbers, [14].

THE OPERATIONAL DESCRIPTION OF SUPERSONIC AIR INTAKE

One of the most important parameters that describe the intake operation efficiency is the total pressure recovery. The total pressure recovery is the ratio of total pressure after compression (behind the normal shock wave) to the free stream total pressure. The air intake operates at “on-design” condition at a certain Mach number, it is called the design Mach number, while it operates an “off-design” condition at any value other than “on-design” Mach number as shown in Figure (3). The inlet area (stream tube capture area at entry) may be defined as the area enclosed by the leading edge, or inlet highlight of the intake cowl, [15]. The maximum flow ratio achievable at supersonic speed occurs when the boundary of the free stream arrives undisturbed at the cowl lip. This means that, $A_{\infty}/A_c=1.0$. The condition will be termed “full flow”. Hence, the maximum flow occurs when the flow remains supersonic up to the entry plane. This means that either normal shock wave is at the cowl lip (starting position) or inside the nozzle, at throat position or just down stream of throat, [14].

DESIGN OF SUPERSONIC AIR INTAKE

This first part of supersonic convergent-divergent nozzle consists of a convergent passage with a sharp inward-facing ramps with a wall deflection angle (δ), as shown in Figure (2). The shocks generated due to the sharp ramps in supersonic flow are called ‘oblique shock waves’. The flow behind the oblique shock is maintained in supersonic flow but at Mach number lower than free stream value. The loss in total pressure across an oblique shock is less than across the normal shock wave. The length of the convergent nozzle (L_1) is very important to design and it is predicted during the estimation of the oblique shock wave reflections, which must be terminated before the throat position, [2].

The first design elements of convergent nozzle are the convergent section length (L_1) and the wall deflection angle (d). The convergent section length of this nozzle may be optimized in terms of total pressure recovery, where all values of pressure recoveries are based on shock losses. These previous elements can be optimized to get intake with following characteristics:-

1. Short enough to avoid the further weights and drags.
2. Long enough to give low loss in the total pressure recovery, [9].

The second part of nozzle consists of diverging passage starts immediately downstream of the converging part. The length of the divergent section (L_2) is very important in design and it is optimized to avoid flow separation. The design elements of divergent nozzle are divergent section length (L_2) and divergence nozzle angle (θ_i). These elements can be optimized to get intake with following characteristics:-

1. Short enough to keep weights and drags to minimum.
2. Long enough to give Mach number range (0.2-0.5) at engine face, [4].
3. The flow reaching engine face must be uniform with high total pressure ratio, avoiding flow separation.

The flow requirement of an existing turbojet engine is used to determine the ranges of entrance to throat area (contraction ratio) variations that are employed in the mechanical design of the model. These area ratios and the shock configuration for optimum pressure recovery at the design point determine the length of the converging part. The length of the rear part is selected so that the maximum

divergence angle at the design condition does not exceed (7°), to avoid flow separation, [6]. This angle is considered to be a reasonable compromise between the requirements of minimum nozzle length and of maximum subsonic nozzle efficiency, [6].

The supersonic convergent-divergent nozzle consists of the following compression processes: -

1. Adiabatic compression process through shock waves
2. Isentropic compression process after normal shock wave.

CONVERGENT-DIVERGENT SUPERSONIC NOZZLE DESIGN ANALYSIS

Several studies have been made in the attempt to optimize such configuration variables as the convergent nozzle length, and divergent nozzle length. For each flight Mach number there is a certain value of nozzle throat section area, then it is important to find the optimum convergent length. In the present design of the internal compression intake, an attempt is made to minimize shock-induced separation by keeping the pressure rise across each shock wave low through small angularity of the internal compression surfaces and multi-shock compression, [15]. The design analysis of this nozzle starts with:-

1. Finding the walls setting angle of the converging part so as to make the oblique shocks from the upper and lower corners (cowl lips) meet at a point that their reflections come to touch the nozzle ramps before the throat position.
2. Determining the oblique shock waves location and their reflections and points of intersection inside the nozzle.
3. Determining the normal shock wave strength and location inside the diverging portion of the nozzle depending on the stagnation pressure ratio across it.
4. Calculating the Mach number distribution along the convergent nozzle after each oblique shock wave.
5. Calculating the stagnation pressure ratio and all other flow properties distribution along the convergent nozzle after each oblique shock wave.
6. Calculating the geometrical dimensions of this nozzle (L_1 , d , L_2 , θ_i).
7. Drawing the whole nozzle with the oblique shock waves and their reflections with the normal shock wave.

CONVERGENT-DIVERGENT NOZZLE DESIGN PROCEDURE

A brief explanation of these calculations are listed in the following steps (1):-
 For an specified engine specifications, let the engine mass flow rate and engine face diameter was assumed equal to ($\dot{m}=60$ kg/sec, $D=58.4733$ cm) respectively. Then the geometrical capture area (A_c) at "on-design" condition ($M_\infty=2.0$), ($H=10000$ m), can be estimated by applying the continuity equation at entry station as follows:-

$$\dot{m} = \rho_\infty \times V_\infty \times A_c \dots (1)$$

where:-

$$V_\infty = M_\infty \times \sqrt{g \times R \times T_\infty} \dots (2)$$

And,

$$\rho_{\infty} = \frac{P_{\infty}}{R \times T_{\infty}} \dots (3)$$

Now by Substituting equations (2) and (3) into equation (1) gives:-

$$\dot{m} = \frac{P_{\infty}}{\sqrt{R \times T_{\infty}}} \times \sqrt{g} \times M_{\infty} \times A_c \dots (4)$$

Where:-

$\dot{m} = 60$ kg/sec, $R = 287$ J/kg.K, $M_{\infty} = 2.0$, $H = 10000$ m, $g = 1.4$.

Then the Mach number at exit station can be calculated by applying mass flow parameter equation between entry and exit stations as follows:-

$$\frac{A_c}{A_e} = \frac{M_e}{M_{\infty}} \left[\frac{1 + \frac{g-1}{2} M_{\infty}^2}{1 + \frac{g-1}{2} M_e^2} \right]^{\frac{g+1}{2(g-1)}} \dots (5)$$

Where, (A_e) is the area at end of convergent - divergent nozzle. The above equation can be solved iteratively using (trial and error method) to find the value of exit Mach number. The exit area (A_e) is equal to the area at engine face (A_f), that may be estimated as follows:-

$$A_f = \frac{p \times D_f^2}{4} = A_e \dots (6)$$

Step: (2) The Mach number of the flow entering the nozzle is the free-stream Mach number, since ($A_{\infty} = A_c$). Hence, for any operating Mach number, there is a maximum value of wall turning angle (δ_{max}) at which an oblique shock solution exists, [3].

Step: (3) To calculate the nozzle throat area needed to start the nozzle, (shock at cowl lips), the following equation can be applied.

$$\frac{A_y}{A_y^*} = \frac{1}{M_y} \left[\frac{2}{g+1} \left(1 + \frac{g-1}{2} M_y^2 \right) \right]^{\frac{g+1}{2(g-1)}} \dots (7)$$

where the throat area required to start the nozzle is calculated by equating the sonic area ratio (A_y/A_y^*) corresponding to subsonic Mach number downstream of normal shock, to the contracting area ratio (A_c/A_{ts}).

Step:(4) To find the nozzle throat area required to operate the intake with a normal condition (normal shock just down stream of throat), the following empirical formula can be applied,[21].

$$\left[\frac{A_{ts}}{A_m} = a + bM + cM^2 + dM^3 + eM^4 + fM^5 + gM^6 \right] \dots (8)$$

Where the confidents of above equation are listed below such that:

a=-0.00673, b=4.8409, c=-8.5311, d=7.1747, e=-3.1144, f=0.691, g=-0.00673.

Step: (5) To find the nozzle wall turning angle (δ that does not exceed δ_{max}), and angle of oblique shock wave (σ), the following equation can be applied, to make the oblique shock and their reflection strikes the nozzle wall surface ahead of the throat position.

$$\frac{\tan (s - d)}{\tan s} = \frac{2 + (g - 1)M_x^2 \sin^2 s}{(g + 1)M_x^2 \sin^2 s} \dots (9)$$

If not, changing the length of the convergent nozzle (L_1) until the above condition is satisfied by re-calculating the step (5) again.

Then the following equation is applied to find the nozzle convergent section length (L_1).

$$\tan d = \frac{(d_c - d_m)}{2} \times \frac{1}{L_1} \dots (10)$$

Step: (6)To calculate the stagnation pressure, Mach number, and all other flow properties distribution after each oblique shock wave or their reflection, the equations of oblique shock waves can be used to calculate these values.

Step: (7)For a given M_1 there is a maximum value of wall turning angle for which the type of reflection known as regular reflection is possible. In other words for a given turning angle (δ) there is a minimum value of M_1 below which regular reflection is impossible. This minimum value of Mach number makes the reflections impossible determined [3].

Step: (8)Continue with calculation for the possible reflections till reaching the minimum Mach number that is determined in the above step.

Step: (9)Update all these reflections and their locations and flow properties, then from the above step the flow Mach number and stagnation pressure after last reflected oblique shock wave had been found, after this point the throat Mach number can be calculated using the following equation:-

$$\frac{A_m}{A^*} = \frac{1}{M_t} \left[\frac{2}{g + 1} \left(1 + \frac{g - 1}{2} M_t^2 \right) \right]^{\frac{g + 1}{2(g - 1)}} \dots (11)$$

Step: (10) The length of the divergent section (L_2) is estimated in the manner similar to that achieved at convergent part, but with maintaining the maximum nozzle wall divergent angle less than 7° (as a limitation to flow separation) from the following equation:-

$$\tan q_i = \frac{(d_e - d_m)}{2} \times \frac{1}{L_2} \quad \dots (12)$$

Step: (11) The stagnation pressure downstream of normal shock is not given at each operating condition from engine manufacturing. Then it is required to compute a value of normal shock Mach number higher than throat value at each operating condition to satisfy the acceptable range of Mach number at engine face (0.2-0.5) with low loss in total pressure recovery, [21].

Then at higher operating Mach number ($M_\infty = 2.5$), the value of throat Mach number close to (1.205), it is desirable to select value of normal shock Mach number higher than this value and it was found close to (1.3), [24].

To find another value of normal shock Mach number at another free-stream Mach number value, it is required to hold a value of ($X_{n.s.w}$) to the corresponding value of above condition ($M_x = 1.3$). Then the area at which the normal shock wave took place (A_x) has been found from the following equation:-

$$\tan q_i = \frac{(A_x - A_x^*)}{2X_{n.s}} \quad \dots (13)$$

Then at each case, the value of normal shock Mach number was changed while remain its position is fixed.

Step: (12) To find each normal shock Mach number at each operating condition apply the following equation:-

$$\frac{A_x}{A_x^*} = \frac{1}{M_x} \left[\frac{2}{g+1} \left(1 + \frac{g-1}{2} M_x^2 \right) \right]^{\frac{g+1}{2(g-1)}} \quad \dots (14)$$

where the choked area (A_x^*) is the geometrical throat area (A_m) and it was estimated in the above steps. The value of stagnation pressure downstream of normal shock can be estimated from the following equation, as follows:

$$\frac{P_{0y}}{P_{0x}} = \left[\frac{2gM_x^2 - (g-1)}{g+1} \right]^{-1} \left[\frac{(g+1)M_x^2}{2+(g-1)M_x^2} \right]^{\frac{g}{g-1}} \quad \dots (15)$$

Step: (13) From the stagnation pressure ratio across a normal shock, the choked area down stream of the normal shock (A_x^*) is calculated from the relation:-

$$\frac{P_{oy}}{P_{ox}} = \frac{A_x^*}{A_y^*} \quad \dots (16)$$

Step: (14) It is desirable to compute the nozzle throat area at “on-design” (when normal shock setting at throat position). When the aircraft fly at Mach numbers other than design value, the normal shock sets at nozzle diverging section. Then to return to the design Mach number value at any Mach number, it is required to bring the normal shock from its position to the throat position, by reducing the geometrical throat area to a value corresponding to sonic area at that Mach number or by equating contraction area ratio (A_c/A_m) with sonic area ratio (A_c/A^*) at intake entry.

Finally a Fortran-95 program was applied to calculate the same above steps and draw the nozzle with the oblique shock waves and their reflections as shown below.

RESULTS AND DISCUSSION

An analytical method is employed to analyze the supersonic inviscid flow through the convergent-divergent nozzle by using the equations of oblique and normal shock waves in the Cartesian coordinate system. In this section the results are concerned with flow properties along the convergent-divergent nozzle at supersonic free stream Mach number (1.6-2.5).

The throat area operating ranges were found equal to (37.509cm -18.304cm) corresponding to free stream Mach number values at off-design operating condition (1.6-2.5) respectively. While the same throat area was found equal to 27.70 cm when the nozzle operates at on-design condition (2.0) as shown in figures and tables below.

Figure (4) presents the Mach number behind the first oblique shock wave as a function of free-stream Mach number for different convergent nozzle length. The oblique shock Mach number increases with increasing of free-stream Mach number for constant convergent nozzle length. This is due to the decrease of oblique shock angle (decrease of shock strength). It increases with increasing convergent nozzle length for constant free-stream Mach number. This is due to the decrease of shock angle (decrease of shock strength).

Figure (5) presents the angle of oblique shock wave as a function of free-stream Mach number for different convergent nozzle length. The angle of oblique shock wave decreases with increasing of free-stream Mach number for constant convergent nozzle length, and it decreases with increasing convergent nozzle length for constant free-stream Mach number. This is due to reducing in wall deflection angle as convergent nozzle length increases (geometrical consideration).

Figure (6) shows the static pressure behind oblique shock wave as a function of free-stream Mach number for different convergent nozzle length. The pressure increases with increasing of free-stream Mach number for constant convergent nozzle length. This is due to the increase of Mach number after first oblique shock wave as free-stream Mach number increasing. It decreases with increasing convergent nozzle length for constant free-stream Mach number. This is occur due to small rise in pressure across each oblique shock as convergent length increases.

Figure (7) shows the total-pressure recovery as a function of free-stream Mach number for different convergent nozzle length. The total-pressure recovery

decreases as free-stream Mach number increases for constant convergent nozzle length. This is due to the loss in total pressure across each oblique and normal shock waves. It decreases rapidly as convergent nozzle length decreases for constant free-stream Mach number. This is due to the increasing of shock strength as nozzle wall turning angle increases.

Figure (8) shows the static pressure distribution respectively along the convergent-divergent nozzle for different free-stream Mach number values. In this figure, the pressure starts to increase from nozzle entrance and continue along each oblique shock wave until reaching at throat position. This is due to the supersonic compression process. Then the pressure starts to decrease along the divergent portion until reaching to normal shock position. This is due to expansion process. Finally, it starts again to increase behind the normal shock wave and continue until reaching to the engine face, and this is due to subsonic compression process. It appears as free-stream Mach number increases the values of these properties increasing. This is due to the increasing of shock strength as free-stream Mach number increases.

Figure (9) presents the Mach number distribution along a whole nozzle for different free-stream Mach number values. The value of each Mach number starts to decrease from nozzle entrance to the throat position. This is due to the supersonic compression process across each oblique shock wave. It increases at a certain distance between the throat position and normal shock wave. This is due to supersonic expansion process. After normal shock, the flow decreases along the divergent passage due to subsonic compression process until, reaching engine face at acceptable Mach number value (0.2-0.5). It appears as the free-stream Mach number increases, the value of Mach number at engine face decreases respectively.

Figure (10) shows the Mach number ahead the normal shock verses the free-stream Mach number for different divergent nozzle length. The upstream Mach number increases with increasing of free-stream Mach number. This occur due to the increasing of Mach number distribution along the nozzle as free-stream Mach number increases. It decreases with increasing of divergent nozzle length for constant free-stream Mach number. This is due the small height of divergent nozzle when shock occurs.

Figure (11) shows the static pressure values down stream the normal shock verses the free-stream Mach number for different divergent nozzle length. The value of pressure increases with increasing of free-stream Mach number value for constant divergent length. The value of pressure decrease with increasing of divergent nozzle length for constant free-stream value. This happened due to the decreasing of shock strength as divergent nozzle length increases.

Figure (12) presents the total-pressure recovery as a function of free-stream Mach number for different divergent nozzle length. The total-pressure recovery decreases as the free-stream Mach number increases for a constant divergent nozzle length. This is true due to the increasing of shock waves strength as the free-stream Mach number increases. The total pressure decreases rapidly as the divergent length decreases for constant free-stream Mach number value. This is due to the increasing of normal shock strength as nozzle divergent length decreases.

Now, Figures. (13), (14), and (15) showing the convergent-divergent supersonic nozzle operating at off-design conditions respectively. It clear there is a

certain number of oblique shock waves (which it induced due to the very sharp inlet cowl lips) at very small nozzle wall turning angle ($\delta=2.4-4.83\text{deg.}$), for a range of Mach number (1.6-2.5) respectively. The length of the convergent nozzle was estimated by the principle of trail and error during the calculation of the oblique shock wave relations. The point is to be reached when the last reflected oblique shock does not cross the throat position. It appears that the length of the convergent nozzle is optimally selected equal to ($L_1=110\text{ cm}$) according to the lowest supersonic Mach number ($M_\infty=1.6$) to avoid further nozzle length and to get acceptable total-pressure recovery. The length of the divergent nozzle is estimated to optimize the nozzle configuration by keeping the nozzle semi-divergent angle below the value that causes the flow separation and to avoid the further length of the whole nozzle. It appears that each reflected shock has the same turning angle (δ) as the first oblique shock, [3]. Because the deceleration through each shock, a point is reached, depending on the initial Mach number (M_∞) and nozzle wall turning angle (δ), beyond which regular reflection is impossible.

The normal shock wave position can be recognized by the red line that shown in these Figures.

The final geometry of the whole nozzle can be summarized as follows: Convergent nozzle length ($L_1=110\text{ cm}$), divergent nozzle length ($L_2=140\text{ cm}$),

Intake entrance height ($d_c=46.74\text{cm}$), intake exit height ($d_e=51.82\text{cm}$), Engine frontal diameter ($D_f=58.47\text{cm}$), distance of normal shock occurrence after throat position ($X_{n.s.w}=5.0\text{ cm}$),

Nozzle divergence angle ($\theta_i=3.45\text{deg.}$)

Finally, Figure (16) shows a convergent-divergent nozzle operates at on-design condition ($M_\infty=2.0$, $H=10000\text{m}$). It appears there is an increase in total pressure recovery over than off-design conditions due to holding the normal shock wave at throat position as shown in Table (4). Then there is no loss in stagnation pressure across the normal shock wave (100%). The position of normal shock at nozzle throat is called (critical location) and will cause the total internal flow pattern to be completely disrupted (intake unstarting), followed by formation of a normal shock ahead of the intake and causes low total-pressure recovery, reduced mass flow through the intake, high spillage drag, and possible engine flameout. Then the normal position of normal shock just down stream of throat it is favorable condition, [3].

CONCLUSIONS

1. This work is associated with analytical solution of the shock wave system (oblique and normal shocks) at supersonic Mach numbers. The program that applied in this research is used successfully to solve equations of shock wave system and find the flow properties along the whole nozzle for compressible, inviscid flow and to predict the optimum design for supersonic internal compression air intake. The following conclusions can be drawn:-

1. In this work the position of normal shock from the throat position is constant which corresponds to ($X_{n.s.w}=5.0\text{ cm}$) for each free-stream Mach number. Then the results show that, as the free-stream Mach number increases causes to increase in

value of upstream Mach number, and as free-stream Mach number increases the total-pressure recovery decreases.

2. The use of nozzle convergent length less than (50 cm), causes no reflection of oblique shock at higher free-stream Mach number ($M_\infty=2.5$), and the use of value exceeding (150 cm) causes extra nozzle weight.
3. The use of nozzle divergent length less than (100 cm), causes high flow separation and return some of flow in opposite direction, and the use of value exceeding (200 cm) causes extra nozzle weight.
4. The nature of geometry form for the convergent-divergent nozzle limits the range of free-stream Mach number (1.6-2.5), to get a specified value of exit Mach number (0.2-0.5), if the free-stream value exceeds (2.5), the corresponding exit Mach number value is less than (0.2). It is found that as the free-stream Mach number increases, the exit Mach number decreases.

REFERENCES

- [1]. DeMarquis, D.W., and Henry, R.S., "An Investigation of Convergent-Divergent Nozzles at Mach Number 1.85", NACA RM E50L07, 1950.
- [2]. Maynard, I.W., "Investigation of Perforated Convergent-Divergent Nozzles with Initial Boundary Layer", NACA RM E50F12, 1950.
- [3]. Shapiro, A.H., "The Dynamics and Thermodynamics of Compressible Fluid Flow", Vol.1, Roland Press, New York, 1953.
- [4]. Abbott, L., and Nettles, J., "Investigation to Mach Number 2.0 of Shock Positioning Control Systems for a Variable-Geometry Inlet in Combination with a J34 Turbo-Jet Engine", NACA RM E54I27, 1954.
- [5]. Emmet, A., and Frank, A., "Experimental Investigation at Mach Numbers from 0 to 1.9 Trapezoidal and Circular Side Inlets for a Fighter-Type Airplane", NACA RM A, 1955.
- [6]. Richard, S., and Warren, E.A., "Investigation of the Performance and Internal Flow of a Variable-Area, Variable-Internal-Contraction", NACA RM A58C24, 1958.
- [7]. Conners, James F., and Meyer, C., "Design Criteria for Axisymmetric and Two-Dimensional Supersonic Inlets and Exits", NACA TN 3589, 1956.
- [8]. John, J., 2004. Mahoney Inlet for Supersonic Missiles, AIAA Education Series, j.s. Przemieniecki. Published by American Institute of Aeronautics, Inc. 370 L, Infant Promenade, SW, Washington, DC. 4.
- [9]. Valorani, M., F.M. Nasuti, 1995. Onofri and C. Buongiorno "Optimal Supersonic Intake Design for Air Collection Engines (ACE), Elsevier Science, 45(12): 729-745.
- [10]. Dr Joe Iannelli, 2006. Calculation of Through Flows in Turbojet Engines and Supersonic Inlets with Flow Control, School of Engineering and Mathematical Sciences City University, Friday, 24 November, 3:30 pm, U316.
- [11]. Lipeman, H.W., A.E. Puckett, 1954. Introduction to Aerodynamics of a Compressible Fluid, Wiley, New York (Glacit Aeronautical Series).
- [12]. Watanabe Y. Aerodynamic Design of 3.5th Configuration Air Intake for Silent Supersonic Technology Demonstrator S3TD. *JAXA Research and Development Memorandum*, JAXA-RM-08-019, 2009.
- [13]. Akatsuka J., Watanabe Y., Murakami A. and Honai S. Porous Bleed Model for Boundary Condition of CFD Analysis. *AIAA paper* 2006-3682, 2006.

- [14]. Anderson, D.A., Tannehill, J.C., and Pletcher, R.H., “Computational Fluid Mechanics and Heat Transfer”, Hemisphere Publishing, New York, 1984.
- [15]. William, W.B., “Fundamentals of Gas Turbines”, John Wiley & Sons, Inc., Canada, 1996.
- [16]. Hill, P.G., and Peterson, C.R., “Mechanics and Thermodynamics of Propulsion”, Addison-Wesley Publishing Co., New Jersey, 1965.
- [17]. Seddon, J. and Goldsmith, E.L., “Intake Aerodynamics”, Collins Professional and Technical Books, William Collins Sons & Co. Ltd. London, 1985.
- [18]. Michel, A.S., “Compressible Fluid Flow”, Prentice-Hall Co., 1985.
- [19]. Emmet, A.M., and Frank, A.P., “An Experimental Investigation at Mach Numbers from 2.1 to 3.0 of Circular-Internal-Contraction Inlets with Translating Center bodies”, NACA RM A56G06, 1956.
- [20]. Nicolai, L.M., “Fundamentals of Aircraft Design”, Addison-Wesley Publishing Co., Ohio, 1969.
- [21]. Mattingly, J.D., “Elements of Gas Turbine Propulsion”, McGraw-Hill Book Co., New York, 1996.
- [22]. Oosthuizen, P.H., and Carscallen, W.E., “Compressible Fluid Flow”, McGraw-Hill Book Co., 1997.
- [23]. Raymer, D.P., “Aircraft Design: A Conceptual Approach”, 2nd Edition AIAA Education Series, Washington, 1992.
- [24]. Mattingly, J.D., Heiser, W.H., and Daley, D.H., “Aircraft Engine Design”, AIAA Education Series, Air Force Institute of Technology, Ohio, 1987.

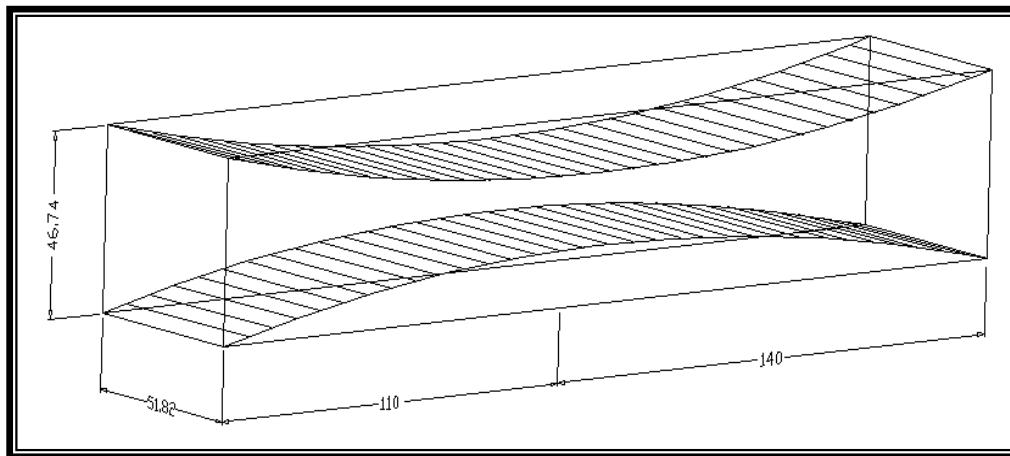


Figure (1) Convergent-divergent supersonic nozzle.

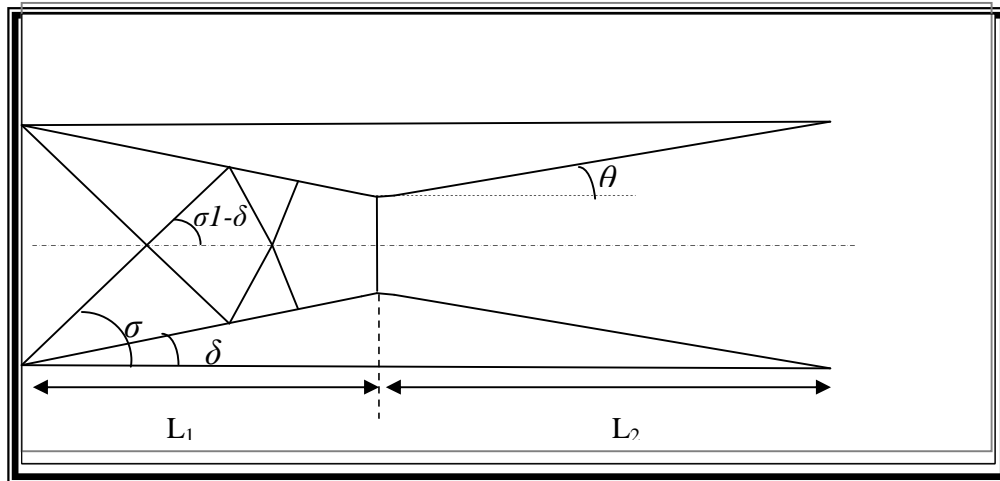


Figure (2) Geometry angles of convergent-divergent supersonic nozzle.

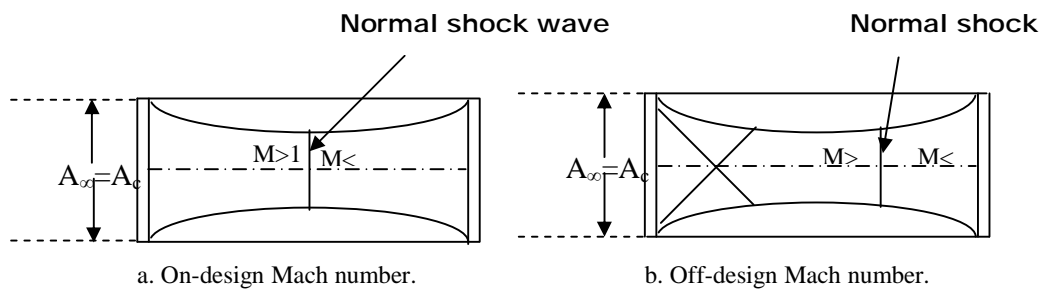


Figure (3) Intake flow operation modes.

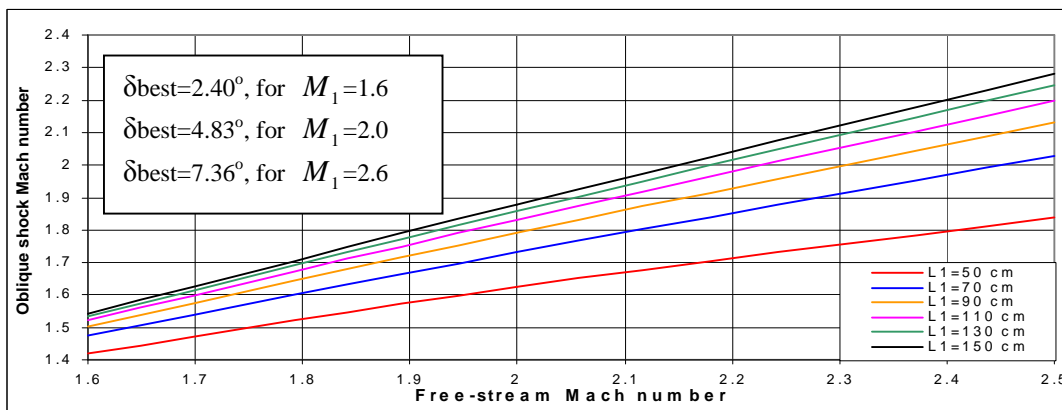


Figure (4) Mach number behind first oblique shock wave versus free-stream Mach number for different nozzle convergent lengths.

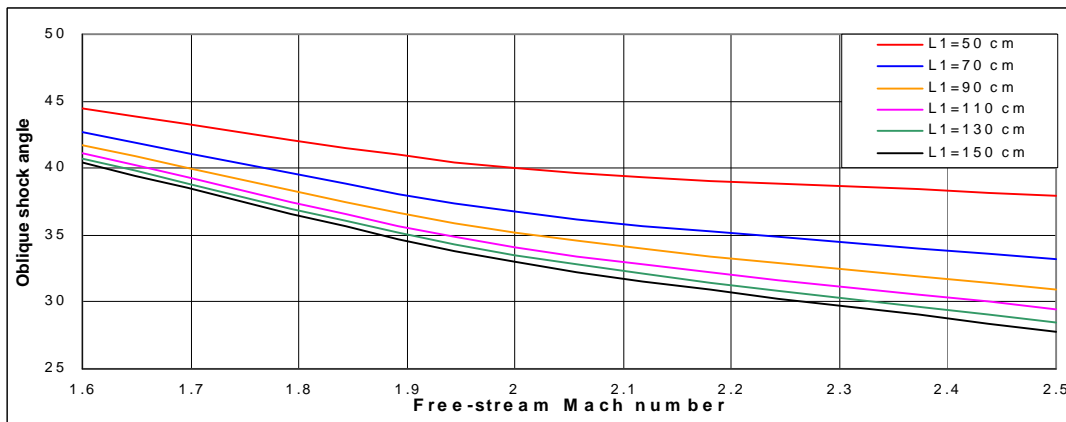


Figure (5) Angle of first oblique shock wave versus free-stream Mach number for different nozzle convergent lengths.

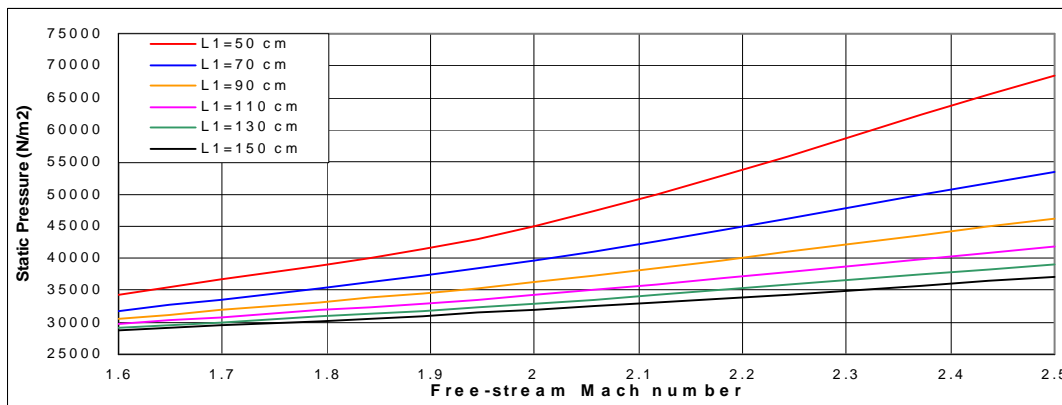


Figure (6) Static pressure behind first oblique shock wave versus free-stream Mach number for different nozzle convergent lengths.

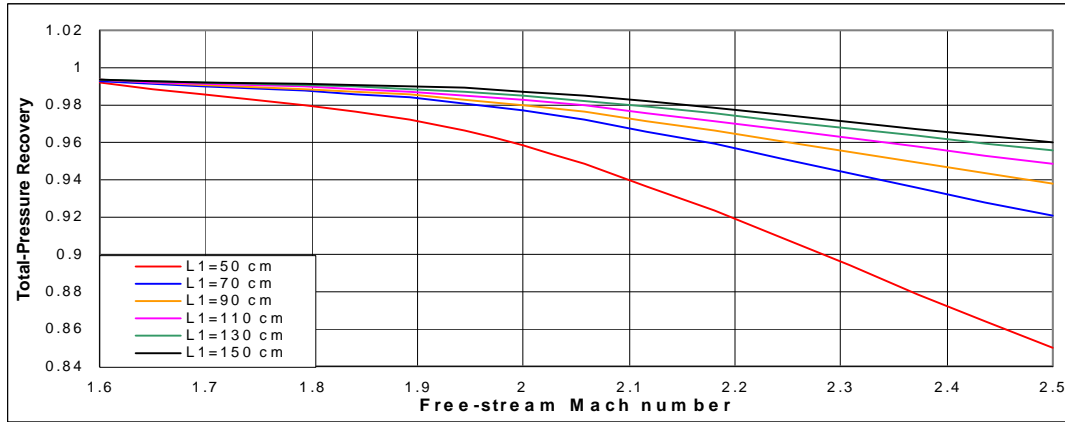


Figure (7) Total-pressure recovery versus free-stream Mach number for different nozzle convergent lengths.

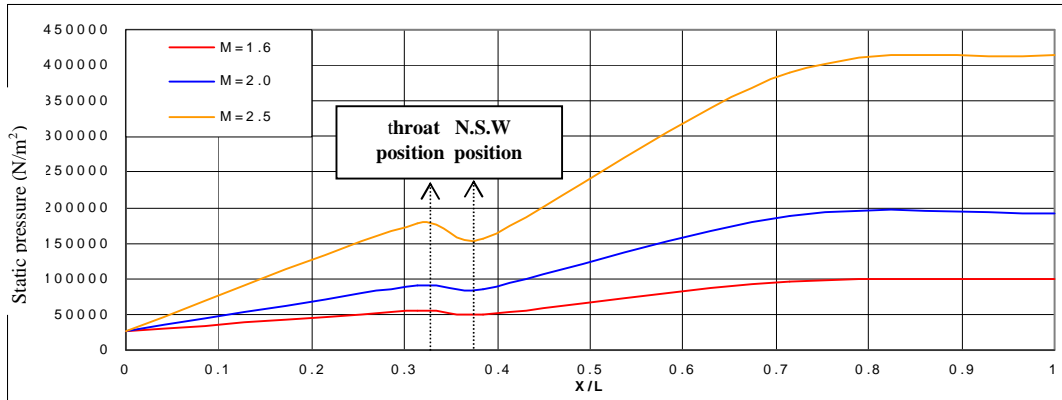


Figure (8) Static pressure distribution along convergent-divergent nozzle for different free-stream Mach numbers.

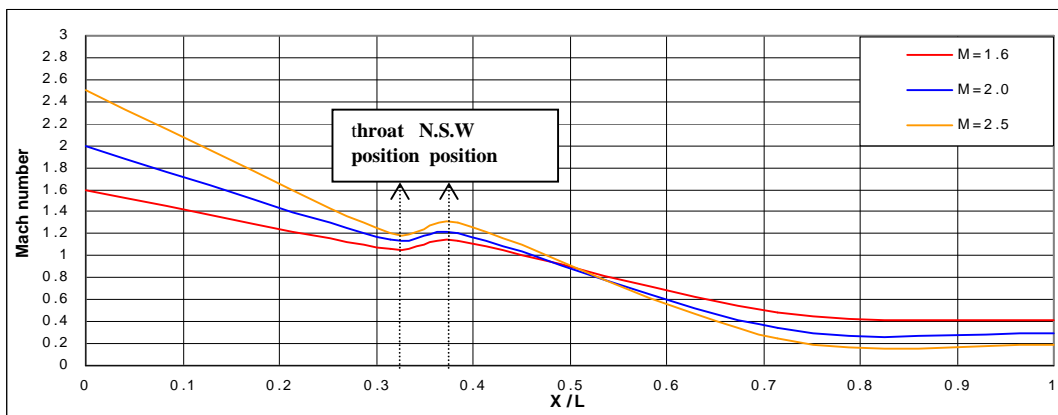


Figure (9) Mach number distribution along convergent-divergent nozzle for different free-stream Mach numbers.

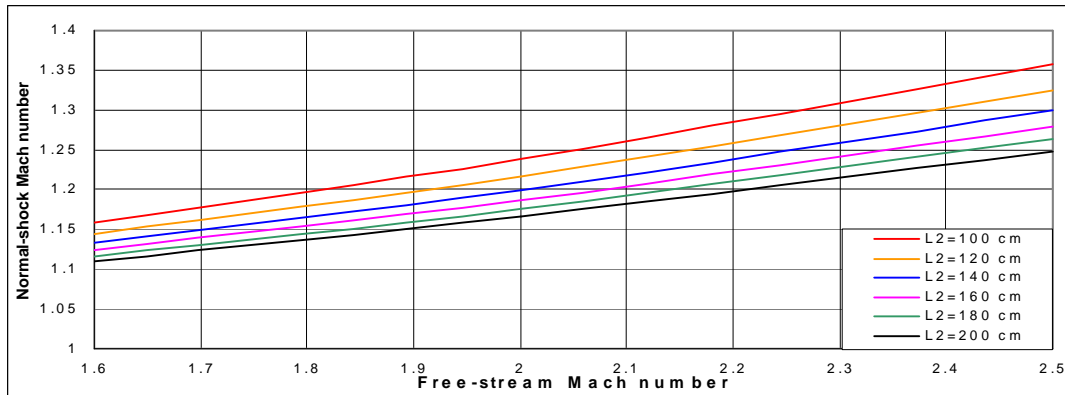


Figure (10) Mach number ahead the normal shock wave versus free-stream Mach number for different nozzle divergent lengths.

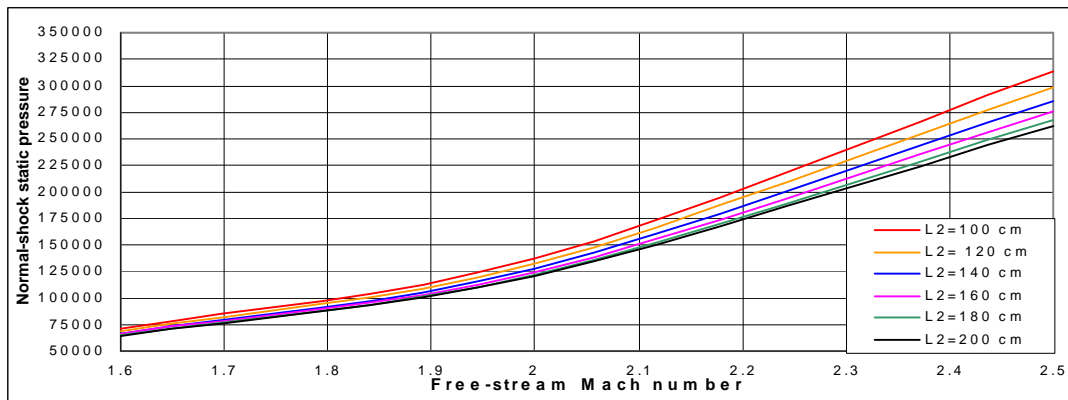


Figure (11) Static pressure downstream the normal shock versus free-stream Mach number for different nozzle divergent lengths.

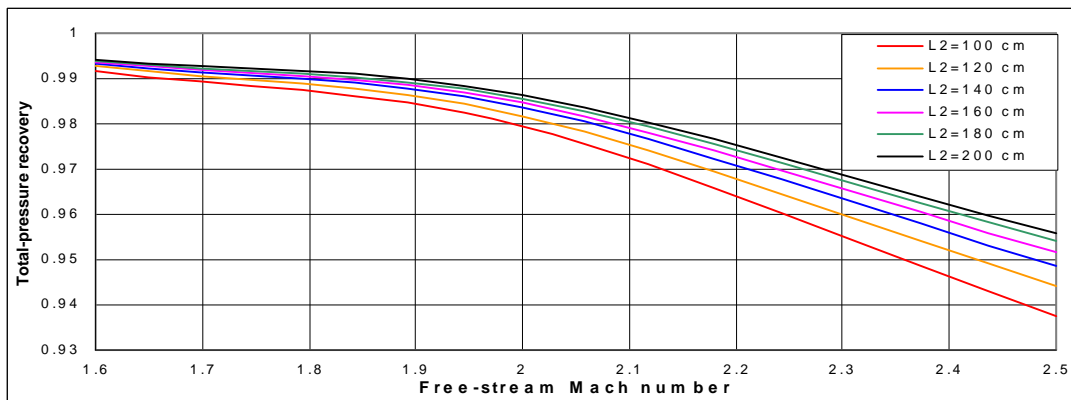


Figure (12) Total-pressure recovery versus free-stream Mach number for different nozzle divergent lengths.

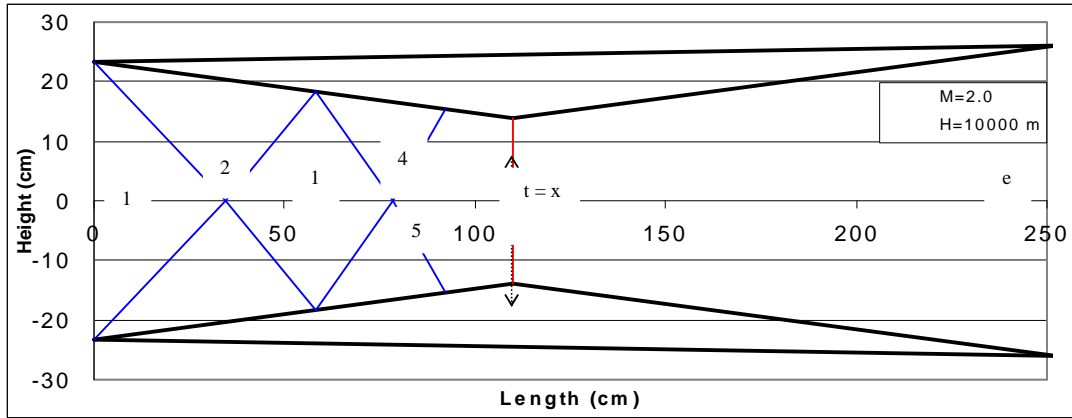


Figure (16) Convergent-divergent supersonic nozzle operates in on-deign condition.

Table (1) Flow properties and Mach number distribution along supersonic air intake.

Properties	δ degree		θ degree		d_t cm			$d_{n.s.w}$ cm			π_N %
		2.4		2.926		37.5			38.03		
Mach no.	M_1	M_2	M_3	M_4	M_5	M_6	M_7	M_t	M_x	M_e	M_f
	1.6	1.521	1.441	1.359	1.273	1.179	1.065	1.06	1.13	0.49	0.42

Table (2) Flow properties and Mach number distribution along supersonic air intake.

Properties	δ degree		θ degree		d_t cm			$d_{n.s.w}$ cm			π_N %
		4.83		4.80		28.159			29.02		
Mach no.	M_1	M_2	M_3	M_4	M_5	M_6	M_7	M_t	M_x	M_e	M_f
	2.0	1.831	1.667	1.505	1.338	-	-	1.145	1.20	0.34	0.29

Table (3) Flow properties and Mach number distribution along supersonic air intake.

Properties	δ degree		θ degree		d_t cm			$d_{n.s.w}$ cm			π_N %
		7.36		6.826		18.3			19.52		
Mach no.	M_1	M_2	M_3	M_4	M_5	M_6	M_7	M_t	M_x	M_e	M_f
	2.5	2.2	1.927	1.67	1.418	-	-	1.205	1.30	0.22	0.202

Table (4) Flow properties and Mach number distribution along supersonic air intake.

Properties	δ degree		θ degree		d_t cm			$d_{n.s.w}$ cm			π_N %
		4.95		4.92		27.7			-		
Mach no.	M_1	M_2	M_3	M_4	M_5	M_6	M_7	M_t	M_x	M_e	M_f
	2.0	1.827	1.659	1.492	1.321	-	-	1.01	-	0.33	0.286

NOMENCLATURE

Symbol	Definition	Units
A	Cross-sectional geometrical area	m^2
A^*	Cross-sectional sonic area	m^2
D	Diameter	m
d	Height of nozzle	m
H	Altitude	m
L_1	Convergent nozzle length	m
L_2	Divergent nozzle length	m
M	Mach number	-
\dot{m}	Mass flow rate	Kg/sec
P	Static pressure	N/m^2
P_0	Stagnation pressure	N/m^2
R	Gas constant	$J/kg.K$
T	Static temperature	K
V	Air flow velocity	m/sec
X	Distance between normal shock and throat	m

Greek letters

Symbol	Definition	Units
δ	Nozzle wall turning angle	deg.
σ	Oblique shock wave angle	deg.
σ_1	Reflected oblique shock wave angle	deg.
Π_N	Total-pressure Recovery	-
r	Air density	Kg/m^3
θ_i	Nozzle internal wall divergence angle	deg.
g	Specific heat ratio	-

SUBSCRIPTS

Symbol	Definition
<i>c</i>	<i>Cowl capture air station</i>
<i>e</i>	<i>End of convergent-divergent nozzle zone</i>
<i>f</i>	<i>Engine frontal area station</i>
<i>t</i>	<i>Nozzle throat station</i>
<i>x</i>	<i>Condition upstream of normal shock wave</i>
<i>y</i>	<i>Condition down stream of normal shock wave</i>
<i>1</i>	Condition before the first oblique shock wave
<i>2</i>	Condition behind the first oblique shock wave
<i>3</i>	Condition behind the second oblique shock wave
<i>4</i>	Condition behind the third oblique shock wave
<i>5</i>	Condition behind the fourth oblique shock wave
<i>6</i>	Condition behind the fifth oblique shock wave
<i>7</i>	Condition behind the sixth oblique shock wave
<i>tn</i>	Geometrical throat position
<i>ts</i>	Geometrical normal shock position
<i>n.s.w</i>	<i>Normal shock wave</i>